MOISTURE CONTENT PREDICTION BELOW AND ABOVE FIBER SATURATION POINT BY PARTIAL LEAST SQUARES REGRESSION ANALYSIS ON NEAR INFRARED ABSORPTION SPECTRA OF KOREAN PINE

Sang-Yun Yang
Graduate Research Assistant
E-mail: sly1357@snu.ac.kr

Yeonjung Han
PhD Candidate
E-mail: jack2001@snu.ac.kr

Yoon-Seong Chang
Graduate Research Assistant
Department of Forest Sciences
Seoul National University
1 Gwanak-ro, Gwanak-gu
Seoul, Korea
E-mail: jang646@snu.ac.kr

Kwang-Mo Kim
Research Scientist
Korea Forest Research Institute
57 Hoegi-ro, Dongdaemun-gu
Seoul, Korea
E-mail: lovewood@forest.go.kr

In-Gyu Choi
Professor
E-mail: cingyu@snu.ac.kr

*Hwanmyeong Yeo**†
Associate Professor
Department of Forest Sciences
Seoul National University
Adjunct Professor
Research Institute for Agriculture and Life Sciences
Seoul National University
1 Gwanak-ro, Gwanak-gu
Seoul, Korea
E-mail: hyeo@snu.ac.kr

(Received May 2013)

* Corresponding author
† SWST member

Wood and Fiber Science, 45(4), 2013, pp. 415-422

Abstract. This study was performed to predict the surface moisture content of Korean pine (*Pinus koraiensis*) with low moisture content (approximately 0%) and high moisture content above the FSP using near IR spectroscopy. Near IR absorbance spectra of circular specimens were acquired at various moisture contents at 25°C. To enhance the precision of the regression model, mathematical preprocessing was performed by determining the three-point moving average and Norris second derivatives. After preprocessing, partial least squares regression was carried out to establish the surface moisture content prediction model. We divided the specimens into two groups based on their moisture contents. For the first group, which possessed moisture contents less than 30%, the R^2 values and root mean squared error of prediction (RMSEP) of the model were 0.96 and 1.48, respectively. For the second group, which possessed moisture contents greater than 30%, the R^2 values and RMSEP of the model were 0.94 and 4.88, respectively. For all moisture contents, the R^2 and RMSEP were 0.96 and 5.15, respectively. As the range of moisture contents included in the prediction model was expanded, the error of the model increased. In addition, the peak positions of the water absorption band (1440 and 1930 nm) shifted to longer wavelengths at higher moisture contents.

Keywords: Near infrared spectroscopy, water absorption band, partial least squares regression, principle component, moisture content measurement.

INTRODUCTION

Logs and sawn timber that have been cut down in the forest contain a large amount of water. Because various defects such as cracks and warps are induced by drying stresses during the drying process, optimization of the drying process is essential for the rational use of green wood. In addition, inappropriate management of the moisture content of wood during storage and transportation causes many problems, which can result in economic loss and decreased wood resource quality. The moisture content of wood-based material must be determined to control physiochemical reactions during painting, adhesion, preservative treatment, and biorefining.

To measure the moisture content of wood in real time, methods based on electrical resistance, electrical capacitance, microwave, and ultrasound have been developed. However, for the electrical resistance method, because the electrical pin is inserted into the measuring point to determine electrical resistance, this procedure produces holes on the surface of the material, and the size of the holes depends on the moisture content and strength of the wood. The presence of holes with variable sizes leads to irreproducible signals and inaccurate moisture content measurements. With other prediction methods, average moisture content of wood can be detected; however, surface moisture content is difficult to measure, which affects the occurrence of surface defects.

In this study, surface moisture content was predicted using near IR (NIR) spectroscopy, which can provide information on the presence of surface water and changes in other chemicals (Tsuchikawa et al 1996b; Tsuchikawa 2007; Eom et al 2010). NIR spectra reflected from the object at wavelengths of 780-2500 nm were used. To achieve an objective quality evaluation without the subjective visual inspection of experts, NIR spectroscopy has been applied in agricultural and food-related industries (Cho 1998; Tsuchikawa 2007). Because characteristics of wood can be measured by NIR spectroscopy without pretreatment such as pelletization, various studies on the correlation between wood and NIR spectra have been performed.

NIR light penetrates deeper than visible light into wood and is easily transmitted through wood (Browne 1957). For sitka spruce, the maximum penetration depth that sufficiently interacts with NIR light is different for each wavelength (Tsuchikawa et al 1996a). Also, longer wavelengths produce lower penetration depths. Tsuchikawa et al (1996b) developed regression models to predict moisture content below the FSP of major Japanese species using NIR spectroscopy.

There were reports that the shifts of NIR absorbance depended on several factors (Czarnik-Matusewicz

and Pilorz 2006; Inagaki et al 2008). In wood science, Thygesen and Lundqvist (2000) reported that the water absorption spectra of wood in the NIR region were shifted because of temperature changes. Because of the previously mentioned phenomena, temperature compensation must be performed on absorption spectra to validate the results.

In this study, an NIR spectroscopic wide-range moisture content prediction model was developed using partial least squares (PLS) analysis. Also, moisture content dependence of the absorption spectra, which were shifted because of variations in the moisture content, was determined.

MATERIALS AND METHODS

Materials

Korean pine (*Pinus koraiensis*) was evaluated in this study. To acquire accurate spectra, the sample must have a sufficient penetration depth, which is the minimum sample thickness in which light is sufficiently diffuse-reflected. Specifically, minimum thickness for sufficient diffuse-reflection decreases with an increase in the wavelength of light. For sitka spruce, which presents an average surface roughness of 8.7 μm, sample thickness should be more than 1 mm at 1100 nm wavelength to negate the effect of thickness (Tsuchikawa et al 1996a).

In this study, with changing thickness of specimens, NIR spectra reflected from the specimens were observed. The reflected NIR spectra did not change when the thickness of specimen was over 5 mm. Fifteen specimens with a thickness of approximately 5 mm were prepared.

Cross-sections were cut from sapwood and their diameter in transversal direction was 40 mm. The cross-section was cut into a circle to minimize the presence of a moisture content gradient at high moisture contents. Because a rectangular shape tends to induce a moisture content gradient at the edges and vertices of the specimen, it is easier to control the moisture content gradient when the sample has a round shape rather than a rectangular shape.

Methods

Below FSP. Specimens were humidified to different moisture contents below the FSP by changing the humidity at a constant temperature of 25°C. The hygrostat used in this study was designed to acquire NIR reflectance spectra in a chamber. After the specimens reached the equilibrium moisture content (EMC) at every RH (Table 1), NIR spectra of the specimens were acquired. Moisture content was determined by the oven-drying method using an electronic scale that had 0.01-g readability and ±0.02-g linearity.

High moisture content. Moisture content was difficult to derive experimentally as the FSP was approached (approximately 30%). However, to construct a regression model including high moisture contents, a moisture content near the FSP must be induced because the FSP is a transition state. To induce a moisture content near the FSP, the thermohygrostat was controlled at 25°C and 100% RH. In these conditions, supersaturated air was supplied into the hygrostat. Supersaturated air is the state that has more vapor pressure than saturated water vapor pressure. We assumed that residual water vapors in supersaturated vapor form droplets at the surface of the wood specimen. Moisture present in the air was condensed on the surface of the specimens. Through this process, moisture contents of the specimens were derived according to the results shown in Table 2.

To obtain a moisture content close to that of green wood, specimens were immersed in a water bath for specified periods of time. After

Table 1. Environmental conditions for humidifying wood specimens below the FSP.

Temperature (°C)	RH (%)	Average EMC (%)	Standard deviation of EMC	Facility
25	99	25.18	1.02	Thermohygrostat
	95	18.20	0.39	
	80	15.30	0.51	
	65	12.90	0.41	
	50	9.70	0.30	
	25	7.64	0.36	
	1	0.76	0.16	

EMC, equilibrium moisture content.

Table 2. Environmental conditions used to achieve moisture contents near the FSP using supersaturated air.

Temperature (°C)	RH (%)	Time (h)	Average MC (%)	Standard deviation of MC (%)	Facility
25	100	4	28.88	1.02	Thermohygrostat
	100	10	32.66	0.39	

Table 3. Soaking conditions used to prepare wet wood specimens above the FSP.

Temperature (°C)	Soaking time (h)	Average MC (%)	Standard deviation of MC (%)	Facility
25	0.5	38.35	2.04	Thermohygrostat
	1	49.40	2.42	
	3	57.59	2.84	
	6	68.42	2.26	
	24	88.45	3.02	

removing the specimens from the water bath, the samples were centrifuged for 5 min at 25°C and 100% RH to prevent water evaporation from the surface and decrease the effects of gravity, which interfere with the uniform distribution of liquid water in the specimen. Table 3 shows the soaking times and corresponding moisture contents.

Chemometric analysis. To acquire the reflectance spectra, a NIR spectrometer (NIR QUEST 256-2.5; Ocean Optics, Dunedin, FL) was used. The instrument was composed of a tungsten halogen lamp (20 W), optical probe, and spectrometer. The spectrometer was calibrated using a standard substance (WS-1-SL; Labsphere) at wavelengths ranging from 1000 to 2400 nm. The optical probe was maintained at 45° when the reflectance spectra were acquired (Fig 1). The diameter detected by the probe was 3 mm. The reflectance data were converted to the corresponding absorbance, and mathematical preprocessing was performed to develop a more precise prediction model. The performed preprocessing treatments included smoothing (three-point moving average) and Norris second gap derivatization (gap size = 1) (Norris 2001). PLS regressions (Geladi and Kowalski 1986) were performed using the Unscrambler (Version 9.7; Camo Inc., Oslo, Norway) in cross-validation mode with a maximum of 20 principal components. In the statistical analysis, several parameters were used to evaluate the reliability of the model. In this study, the coefficient of determination (R^2) and root mean square error of prediction (RMSEP) of each model were compared.

The PLS regression model could be written as Eq 1 (Rännar et al 1994):

$$Y = XB + F \quad (1)$$

In Eq 1, Y is a dependent variable, X is an independent variable, B is a regression coefficient, and F is an error term. Eq 1 could be exchanged for a wood moisture content prediction model. In this case, Y, X, and B can be changed to moisture content of specimen, $X_{\lambda i}$, and B_{PCn}, respectively, as in Eq 2.

$$MC = X_{li}B_{PCn} + F \quad (2)$$

In Eq 2, $X_{\lambda i}$ is spectrum value at λ_ith wavelength; the dimension of B_{PCn} is differed by number of principle component (PC). Each variable was expressed by a matrix.

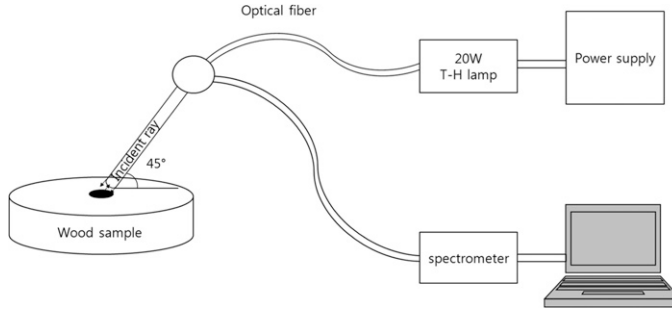

Figure 1. Experimental setup used to measure the reflectance spectra of specimens.

RESULTS AND DISCUSSION

Dependence of Water Absorption Bands on Moisture Content

The original absorption spectra and preprocessed spectra of each moist specimen are shown in Fig 2a and b, respectively. In Fig 2a, absorbance at 1440 and 1930 nm increased with increase in moisture content. These absorption bands were transformed into negative peaks after obtaining the second derivatives (Fig 2b). In this study, PLS analysis was conducted to obtain the second derivative of the absorbance spectra. Spectroscopic interpretations of preprocessed spectra must be performed. As shown in Fig 2b, the peaks at 1930 and 1440 nm moved to a lower wavelength as moisture content increased, and the negative peak at 1440 nm in the second derivative absorbance spectra moved to 1422 nm as moisture content increased. Similarly, the negative peak at 1930 nm moved to 1900 nm as moisture content increased. These results indicated that the peak positions of the water absorption bands shifted because of changes in the moisture content of wood.

Near IR Model Analysis

Figure 3 shows the validity of the moisture content prediction model below the FSP using preprocessed spectra (Fig 3a) and the regression coefficients for each PC (Fig 3b). Moisture contents below the FSP only included the states shown in Table 1. For predicting moisture contents below the FSP, the model showed high correlations ($R^2 = 0.96$, RMSEP = 1.48) and contained three PCs after optimization. However, relatively high prediction errors occurred for the 0.76% EMC group, which was conditioned at 1% RH. Because of the high prediction error, we analyzed the regression coefficients of each principal component and spectral characteristic.

As shown in Fig 2a, the absorbance of light by wood, especially light at wavelengths of 1440 and 1930 nm, which are the absorption bands of water, increased with an increase in moisture content in the hygroscopic range. In contrast, dried wood humidified at 1% RH barely absorbed light.

Based on the high absolute values of the regression coefficients for each component, water absorption bands can be used to predict the moisture content of moist specimens but not those of dried specimens humidified at 1% RH.

The previously mentioned results may be attributed to the fact that the regression coefficients for each principal component appeared as negative peaks at wavelengths of 1422 and 1913-1919 nm. Additionally, the peak position moved to shorter wavelengths as the number of PC increased.

As shown in Fig 4, the positions of the negative peaks in the second derivative spectra moved

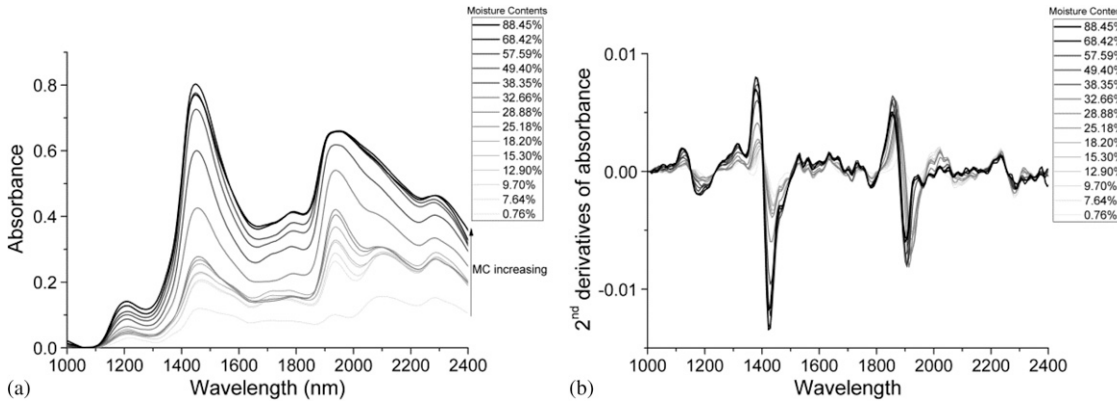

Figure 2. Absorbance spectra: (a) original absorbance spectra, (b) preprocessed absorbance spectra (three-point moving average, Norris second derivative [gap size = 1]).

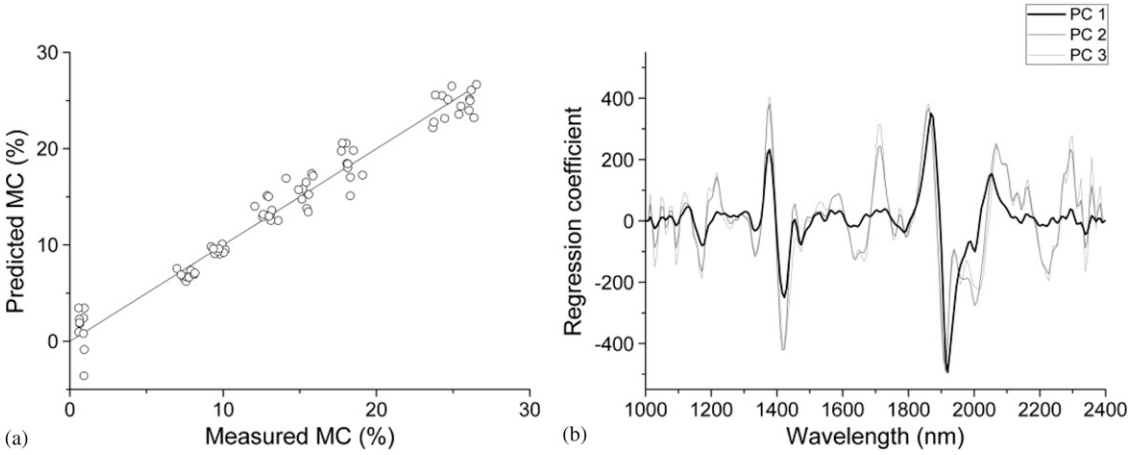

Figure 3. Surface moisture content (MC) prediction model below the FSP, which was developed by partial least squares analysis with preprocessed near IR spectra: (a) validation result, (b) regression coefficients for each principal component (PC).

from 1441 to 1435 nm and 1932 to 1919 nm when moisture content increased.

Figure 5 shows the validation results of the regression model for high moisture contents and the corresponding regression coefficients. The moisture content predicted by the model, which contained seven PCs after optimization, presented a high correlation with the actual moisture content, although the error was high ($R^2 = 0.94$, RMSEP = 4.88). The RMSEP of the prediction model for high moisture contents was higher than that of moisture contents below the FSP. The observed increase in error caused by an increase in moisture content was attributed to two primary causes.

First, for high moisture contents, the moisture content of the spectra acquisition point may be different from that of the average moisture content of the specimen. To obtain a uniform high moisture content, specimens were soaked in a water bath for a long time and were subjected to a centrifuging process to obtain a uniform moisture content distribution in the specimen. Nevertheless, differences between the moisture content of the NIR acquisition point and average moisture content of specimens may be inevitable.

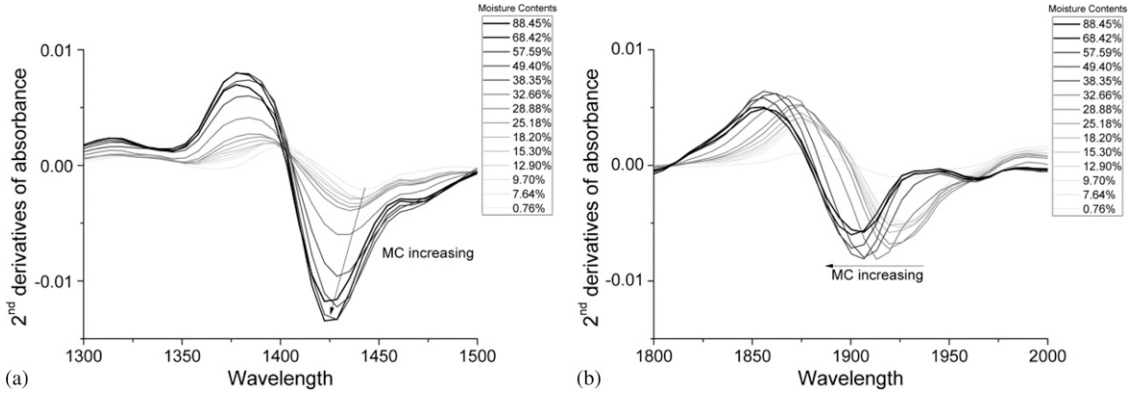

Figure 4. Preprocessed absorbance spectra (three-point moving average, Norris second derivative [gap size = 1]): (a) 1440-nm band, (b) 1930-nm band.

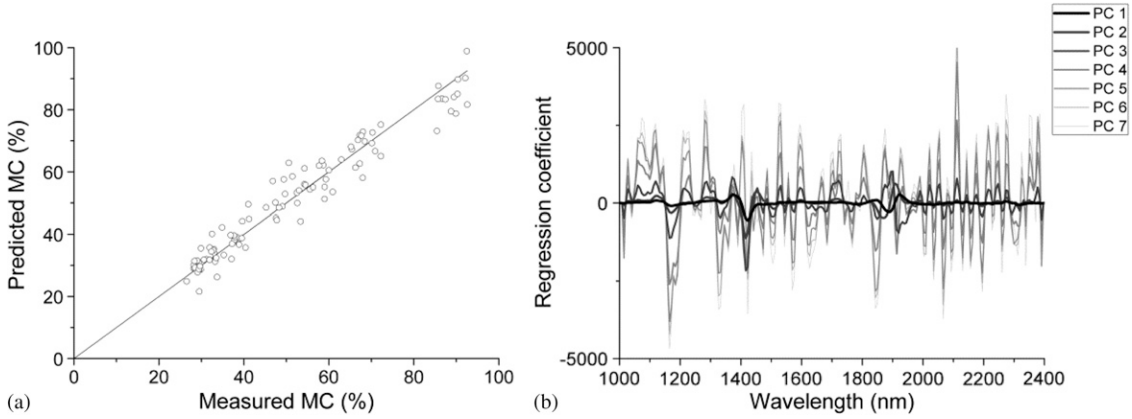

Figure 5. Surface moisture content (MC) prediction model above the FSP developed by partial least squares analysis with preprocessed near IR spectra: (a) validation result, (b) regression coefficients for each principal component.

Second, gaps occurred between the peak positions of the regression coefficients at each principal component (Fig 5b) and water absorption band (Fig 4b). Although the negative peak position at 1930 nm in the second derivatives spectra moved to shorter wavelengths when the moisture content increased (Fig 4b), the regression coefficients of PC1, PC2, and PC3 showed positive peaks at 1919, 1906, and 1900 nm, respectively (Fig 5b). The peak positions of the regression coefficients for each PC of prediction model above FSP showed opposite signs and displayed wider shifts compared with those of the prediction model below the FSP (Fig 3b).

Negative peaks of regression coefficients of the model above FSP occurred at 1416 nm, which represented a 6-nm wavelength difference compared with those obtained below the FSP, which occurred at 1422 nm. The observed difference may be caused by shifts in the water absorption peak in the second derivatives spectra, which were attributed to changes in the moisture content level.

Figure 6 shows the validation results of the moisture content prediction model for the entire moisture content range of wood (Tables 1, 2, and 3) using preprocessed spectra (a) and regression coefficients of the model at each PC (b).

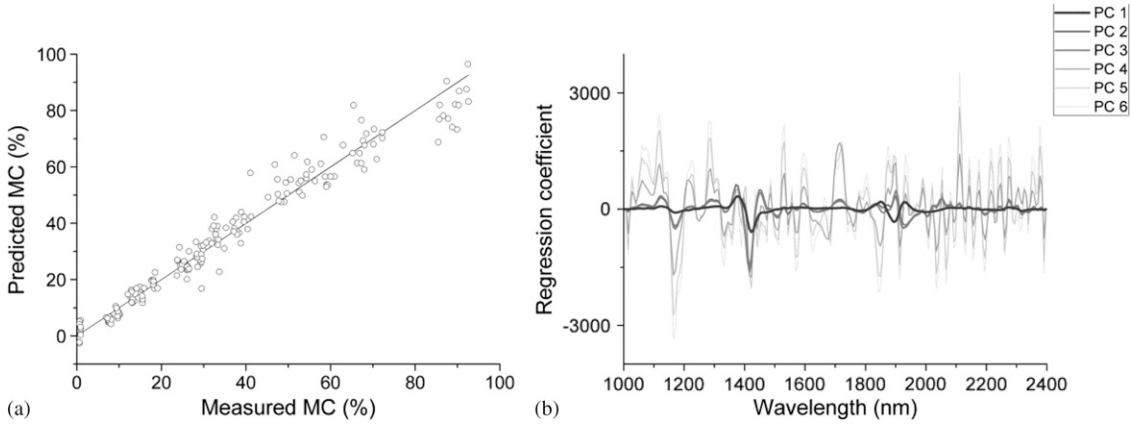

Figure 6. Surface moisture content (MC) prediction model for the entire MC range, which was developed by partial least squares analysis with preprocessed near IR spectra: (a) validation result, (b) regression coefficients for each principal component.

The moisture content predicted by the model, which contained six PCs after optimization, presented a high correlation with the measured moisture content, although the error was high ($R^2 = 0.96$, RMSEP = 5.15). The RMSEP of the prediction model for all the moisture contents was higher than that of moisture contents below the FSP. The root cause of the high error may be similar to that of the high moisture content prediction model.

We analyzed the regression coefficients of all the moisture content models from PC1 to PC3 (Fig 6b). For the 1440-nm absorption band, a significant shift in the peaks of the regression coefficients was not observed. In contrast, the regression coefficients at 1930-nm absorption band showed a positive peak for PC1 (1932 nm) and negative peaks for PC2 (1925 nm) and PC3 (1932 nm).

In the second derivative spectra, the water absorption bands shifted from 1932 to 1900 nm and 1440 to 1422 nm as moisture content increased. These shifts may have resulted in significant errors.

CONCLUSION

In this study, we confirmed that surface wood moisture contents could be predicted using NIR spectra at wavelengths of 1000-2400 nm when the moisture content was less than 100%. The peaks of preprocessed absorbance spectra shifted as moisture content increased. As a result, as the range of moisture contents within the prediction model expanded, the RMSEP increased. However, the R^2 values did not show the same tendency. Therefore, to develop a more concise moisture content prediction model, shifts in the peaks of preprocessed absorbance spectra should be considered. Calibration of the observed peak shift may improve the validity and reliability of the proposed moisture content prediction model.

ACKNOWLEDGMENT

This research was supported by the Basic Science Research Program of the National Research Foundation of Korea (NRF), which is funded by the ministry of Education, Science and Technology (2011-0003453).

REFERENCES

Browne F (1957) The penetration of light into wood. Forest Prod J 7:308-314.

Cho KC (1998) Application to agricultural study of near infra red spectroscopy. Korean Society for Agricultural Machinery 23(2):195-205.

Czarnik-Matusewicz B, Pilorz S (2006) Study of the temperature-dependent near-infrared spectra of water by two-dimensional correlation spectroscopy and principal components analysis. Vib Spectrosc 40(2):235-245.

Eom CD, Han Y, Chang Y, Park JH, Choi JW, Choi IG, Yeo H (2010) Evaluation of surface moisture content of *Liriodendron tulipifera* wood in the hygroscopic range using NIR spectroscopy. Journal of the Korean Wood Science and Technology Mokchae Konghak 38(6):526-531.

Geladi P, Kowalski BR (1986) Partial least-squares regression: A tutorial. Anal Chimica Acta 185:1-17.

Inagaki T, Yonenobu H, Tsuchikawa S (2008) Near-infrared spectroscopic monitoring of the water adsorption/desorption process in modern and archaeological wood. Appl Spectrosc 62(8):860-865.

Norris KH (2001) Applying Norris derivatives. Understanding and correcting the factors which affect diffuse transmittance spectra. NIR News 12(3):6.

Rännar S, Lindgren F, Geladi P, Wold S (1994) A PLS kernel algorithm for data sets with many variables and fewer objects. Part 1: Theory and algorithm. J Chemometr 8(2):111-125.

Thygesen LG, Lundqvist SO (2000) NIR measurement of moisture content in wood under unstable temperature conditions. Part 1. Thermal effects in near infrared spectra of wood. J Near Infrared Spectrosc 8(3):183-190.

Tsuchikawa S (2007) A review of recent near infrared research for wood and paper. Appl Spectrosc 42(1):43-71.

Tsuchikawa S, Hayashi K, Tsutsumi S (1996a) Nondestructive measurement of the subsurface structure of biological material having cellular structure by using near-infrared spectroscopy. Appl Spectrosc 50(9):1117-1124.

Tsuchikawa S, Torii M, Tsutsumi S (1996b) Application of near infrared spectrophotometry to wood, 4: Calibration equations for moisture content. Journal of the Japan Wood Research Society (Japan) 42(8):743-754.